Patterned turbulence and relaminarization in MHD pipe and duct flows

Dmitry Krasnov[1], Oleg Zikanov[2] and Thomas Boeck[1]

[1]Institute of Thermodynamics and Fluid Mechanics, Ilmenau University of Technology, 98684 Ilmenau, Germany

[2]Mechanical Engineering, University of Michigan - Dearborn, USA

Abstract

We present results of a numerical analysis of relaminarization processes in MHD duct and pipe flows. It is motivated by Julius Hartmann's classical experiments on flows of mercury in pipes and ducts under the influence of magnetic fields. The computed critical parameters for transition as well as the friction coefficients are in good agreement with Hartmann's data. The simulations provide a first detailed view of flow structures that are experimentally inaccessible. Novel flow regimes with localized turbulent spots near the side walls parallel to the magnetic field are observed.

Introduction. The processes of flow re-laminarization in tubes (i.e. pipes and ducts) were the first MHD phenomena studied experimentally by the work of Hartmann & Lazarus (1937). The experimental settings were pipes and ducts of different aspect ratios, subjected to a uniform transverse magnetic field. The flows had moderate values of the Reynolds number and magnetic fields B. Laminarization was detected by comparing the measured pressure drop with theoretical values based on laminar MHD channel flow. The transition threshold could be associated with a certain value of the Reynolds number R based on the thickness of the laminar Hartmann layer. However, theoretical works have not been able to give a satisfactory explanation of transition in the MHD tube flows so far. One reason for this is the particular structure of the laminar velocity distribution in tube flows, which is characterized by a flat core and thin electromagnetic boundary layers. The Hartmann layers form at the walls perpendicular to the magnetic field and have a thickness $\sim 1/B$. On the walls parallel to the field there are corresponding side layers called Shercliff layers (in rectangular ducts) or Roberts layers (in circular pipes). They are thicker than the Hartmann layers and have a different scaling with B. Since the shear is concentrated in Hartmann and side layers, they may both support instabilities leading to turbulence. The role of R as decisive parameter for transition points to the Hartmann layers as origin of transition. However, there are indications that instability first develops in the side layers, e.g. by an analysis of optimal linear perturbations in MHD duct flow (Krasnov *et al.* (2010)). In the present work we therefore examine relaminarization by direct numerical simulations of MHD tube flows for the parameters of the experiments by Hartmann & Lazarus experiments and extend them to higher Reynolds numbers and stronger fields. Our contribution mainly focuses on results from Krasnov *et al.* (2013) and Zikanov *et al.* (2013).

Mathematical model and numerical method. We consider flows of incompressible, Newtonian, electrically conducting fluids (e.g. liquid metals) in rectangular duct or circular pipe. The flow is subjected to a uniform magnetic field B_0. Based on the assumption of small magnetic Reynolds number Re_m, the flows are described by the quasi-static approximation of MHD equations Davidson (2001). The governing non-dimensional equations and boundary conditions are given in Krasnov *et al.* (2013). The non-dimensional parameters are the Reynolds $Re \equiv Ua/\nu$ and Hartmann $Ha \equiv Ba\,(\sigma/\rho\nu)^{1/2}$ numbers. Here U is the mean flux velocity, a is the half-diameter (pipe) or half-height (duct), σ is the electrical conductivity.

The governing equations are solved numerically by our in-house DNS solvers, implemented for rectangular (duct) and cylinder (pipe) geometries. The solvers are based on finite-difference method described in Krasnov *et al.* (2011). The spatial discretization of 2^{nd} order is on a non-uniform structured grid formed along the lines of the Cartesian (duct) or cylindrical (pipe) coordinate system. The time integration is explicit and uses projection-correction procedure to satisfy incompressibility. The computational grid can be clustered in the wall-normal (or radial) directions to provide adequate resolution of the boundary layers.

Results and discussion. The simulations have been conducted for two settings: flows periodic in the streamwise direction and flows with non-periodic inlet/exit conditions. Periodic conditions represent a fully developed flow under perfectly uniform magnetic field. The non-periodic formulation, on the other hand, is more realistic and allows us to apply non-uniform magnetic fields with sharp gradients at the entry and exit of the test sections. By that it is possible to mimic the real flow conditions in experiments, where the magnetic field is never perfectly uniform and the flow evolution is influenced by entry effects.

The specific focus of our study, apart from reproducing the classical MHD experiments Hartmann & Lazarus (1937), is on the appearence of patterned turbulence in MHD tubes. The phenomenon of patterned turbulence, i.e. coexistence of laminar and turbulent zones, is known for hydrodynamic wall-bounded shear flows, e.g. puffs and slugs in pipe flow (Reynolds, 1883; Wygnanski & Champagne, 1973) and spiral bands in Taylor-Couette flow (Andereck *et al.*, 1986). However, coexistence of stable laminar and turbulent regions has not been directly demonstrated for MHD tube flows.

Simulations of periodic duct and pipe flows. We start with the results of periodic DNS (Krasnov *et al.*, 2013), where flows in a pipe and a duct of square cross-section are analyzed at moderate (3000 to 5000) values of Re. The key feature of these simulations is the large length of the computational domain, up to 64π in terms of the hydraulic radius a. As a result of that, previously unknown patterned turbulence regimes have been observed for both pipe and duct. The regimes are realized in all DNS conducted within a certain range of Ha (e.g., at $Re = 5000$, the range was $21 < Ha < 26$ for duct and $18 < Ha < 23$ for pipe). This range of Ha is found to be the transitional one. Below and above it, all the simulations yield fully turbulent or fully laminar flows.

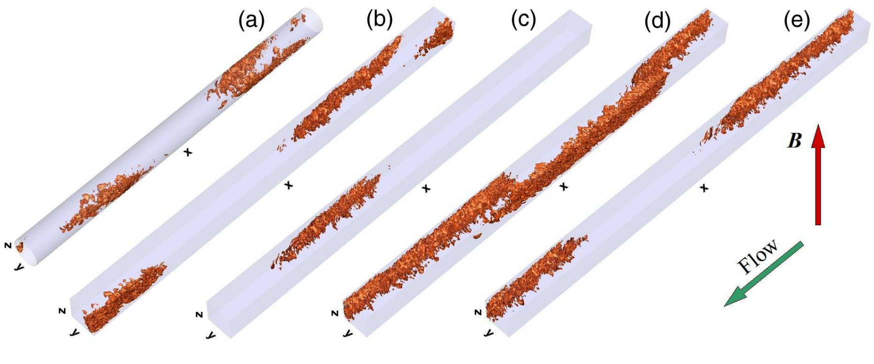

Figure 1: Patterned turbulence regimes in pipe and duct flows in periodic domains. Different flow states at $Re = 5000$ are visualized by iso-surfaces of turbulent kinetic energy of transverse velocity components: puffs in pipe at $Ha = 22$ (a), double- and single-sided puffs in duct at $Ha = 25$ (b, c), and extended turbulent zones induct at $Ha = 22$, cases of double- and single-sided patterns (d, e). The total length of the computational domain is 80 pipe radii in (a) and 32π of duct half-widths in (b)-(e).

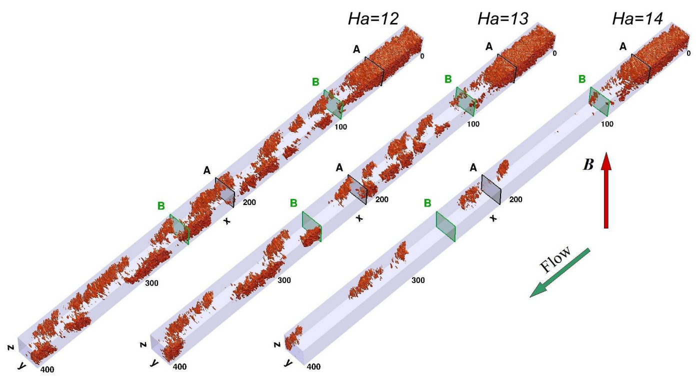

Figure 2: Patterned turbulence in spatially evolving duct flows. The isosurfaces of TKE of the transverse velocity components corresponding to 2% of the maximum are shown. Flows under stepwise magnetic field at $Re = 3000$ are visualized for $Ha = 12$, 13 and 14. (A–A) and (B–B) indicate the pressure measurement sections, the upstream location (A) also shows the point where the magnetic field begins.

The patterned turbulence regimes are illustrated in figure 1. We can see that the flow in the core and Hartmann boundary layers remains essentially laminar. The puffs localized in the sidewalls tend to form staggered patterns (fig. 1b,d) although the specific arrangement is largely influenced by initial conditions. We have also analyzed the temporal evolution of the puffs and identified multiple events as, e.g., merging and splitting of two or more neighboring puffs, two opposite-side spots forming a 'locked' state and traveling together (fig. 1a). In most cases one can identify a characteristic length of a single spot, which is about 30 radii.

Patterned turbulence in spatially evolving MHD duct and pipe flows. We have also made an attempt to reproduce the real experimental conditions of the Hartmann setup. To do so we have performed more realistic transition simulations at $Re = 3000$ with in- and outflow conditions (see Zikanov *et al.* (2013)). Turbulent conditions at the inlet are obtained from a periodic flow simulation running at the same Re and grid spacing. The streamwise domain-size was chosen as $L_x = 128\pi$ to minimize the effects of exit boundary conditions and to provide more room for the spatial evolution of turbulent spots.

The results of these runs confirm the general conclusions from the simulations with periodic boundary conditions. Fig. 2 shows a typical spatial development of the flow in this case. Here the first streamwise section marked as A indicates the position where the magnetic field begins. Downstream of this position the turbulent fluctuations are reduced by the magnetic damping and both Hartmann layers and the bulk of the duct become laminar. At $Ha = 12$ turbulence is still maintained in extended zones located near the Shercliff walls. At $Ha = 13$ we observe the appearance of relatively stable puffs of well-defined length with a tendency to arrange in a staggered pattern. At $Ha = 14$ the magnetic damping is already too strong to sustain regular pattern of turbulent puffs, however weak spots are still generated occasionally at one of the Shercliff walls. Finally, at $Ha = 15$ the flow becomes essentially laminar at the first position marked B, although sporadic events can appear, but these spots die out quickly.

The only available parameter from the Hartmann experimental study was the average pressure gradient dp/dx between two manometers, which can be recalculated in the friction coefficient $f = 2a\, dp/dx/(\rho U^2)$. We, therefore, have also measured f for both periodic and non-periodic simulations to compare with the experiments. Fig. 3 shows that the friction coefficients agree well between experiments and periodic and non-periodic simulations. Upon increasing Ha the friction is initially reduced because of the magnetic damping of turbulence. For $Ha > 15$ it increases linearly with Ha because friction in the laminar Hartmann layers becomes the dominant contribution. Relaminarization occurs close to the minimum of the friction coefficient. In experiments this has typically been found for a parameter

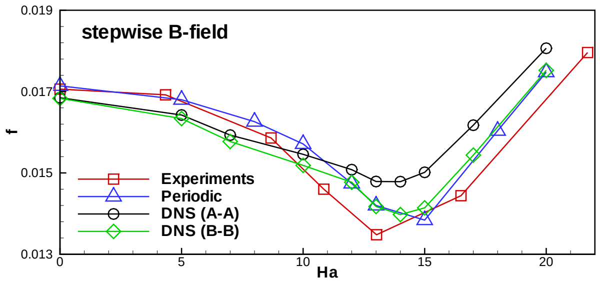

Figure 3: Friction coefficient vs. Hartmann number Ha shown for the results of simulations and experimental data (Hartmann & Lazarus, 1937).

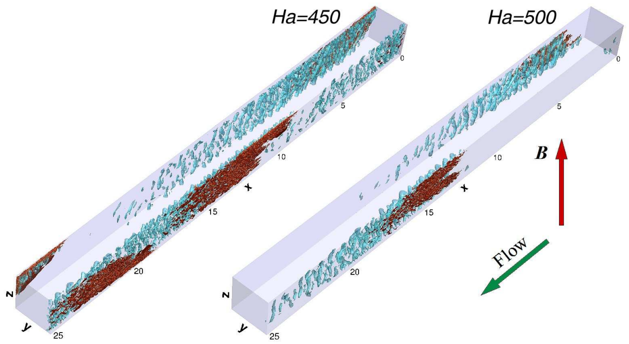

Figure 4: Patterned turbulence regimes realized in simulations of duct flow at $Re = 10^5$ and $Ha = 450,\ 500$. The isosurfaces of TKE (brown) of transverse velocity components corresponding to 2% of the maximum are shown, also shown are the isosurfaces of the second eigenvalue λ_2 (cyan) of tensor $S_{ik}S_{kj} + \Omega_{ik}\Omega_{kj}$.

$R = Re/Ha \approx 200$.

Patterned turbulence in MHD duct at high Re and Ha. The numerical simulations at low and moderate Re and Ha suggest that similar spots can also be expected in the transitional range of Ha at higher Re. So far such regimes have not been observed in our prior study of MHD duct flow at $Re = 10^5$ (Krasnov *et al.*, 2012). This can be attributed to the insufficient length of computational domain $L_x = 4\pi$. To verify this hypothesis we have conducted a series of simulations, in which the length L_x has been increased to 8π. However, the results should be viewed as preliminary because we used a coarser computational grid with $N_x \times N_y \times N_z = 2048 \times 385^2$, i.e. with steps two times larger than in Krasnov *et al.* (2012).

The results are illustrated in figure 4 for $Ha = 450$ and 500 that correspond to the transitional range of $R = Re/Ha \approx 200$. The flow is laminar in the core and the Hartmann boundary layers, but has strongly pronounced turbulent spots near the sidewalls. At $Ha = 450$ ($R = 222$, left plot) the puffs are already isolated and maintain their identity, approximate energy, and approximate length for the entire duration of the simulation. These puffs are similar to those observed earlier in MHD pipe and duct at lower Re and Ha (Krasnov *et al.*, 2013; Zikanov *et al.*, 2013). A typical puff length calculated in terms of the Shercliff layer thickness δ_{Sh}, is $L_{puff}/\delta_{Sh} \approx 130 - 150$. This is consistent with the results at lower Re and Ha, where the puff length of 30 radii amounts to $L_{puff}/\delta_{Sh} \approx 125 - 150$. At higher Ha most of our attempts have ended in fully laminar flow states. However, one simulation started with a realization at $Ha = 450$ has produced a regime with two isolated turbulent spots showing no tendency to further decay. The isolated puffs at $Ha = 500$ ($R = 200$, right plot in fig. 4) have significantly lower turbulent kinetic energy than the puffs at $Ha = 450$ and smaller length: $L_{puff} \approx 85\delta_{Sh}$.

Summary and conclusions. DNS of MHD duct and pipe flows have been performed to reproduce the classical laminarization experiments by Hartmann Hartmann & Lazarus (1937). One distinct feature is the co-existence of laminar and turbulent regions at the edge of laminarization. The peculiarity of the MHD flows is the localization of these turbulent zones in the sidewall layers. The friction coefficients measured by Hartmann are in good agreement with our DNS. It is, however, important to notice that this integral parameter provides no indication of the existence of turbulent zones as their impact on the total friction is very low. We also notice that at high $Ha \approx 450$ ... 500 the appearance of isolated puffs is accompanied by the quasi-$2D$ columnar vortices (cyan shading in fig. 4), identified earlier in our study (Krasnov *et al.*, 2012). It seems plausible that there is an interaction between the puffs and quasi-$2D$ vortices, such that the puffs are stretched along the magnetic field direction and resemble objects known as "turbulent bands". Further work is necessary to resolve the details of transition in the side layers and to explain why the parameter R determines the transition in a wide range of Re and Ha numbers.

Acknowledgements. TB and DK acknowledge financial support from the Helmholtz Alliance "Liquid Metal Technologies" and the Deutsche Forschungsgemeinschaft. OZ acknowledges financial support from the U.S. National Science Foundation (Grants CBET 0966557 and CBET 1232851). Computer resources were provided by the computing centers of Forschungszentrum Jülich (NIC) and TU Ilmenau.

References

Andereck, C. D., Lui, S. S. & Swinney, H. L. 1986 Flow regimes in a circular couette system with independently rotating cylinders. *J. Fluid Mech.* **164**, 155–183.

Davidson, P. A. 2001 *An Introduction to Magnetohydrodynamics*. Cambridge University Press.

Hartmann, J. & Lazarus, F. 1937 Hg-dynamics II: Experimental investigations on the flow of mercury in a homogeneous magnetic field. *K. Dan. Vidensk. Selsk. Mat. Fys. Medd.* **15** (7), 1–45.

Krasnov, D., Thess, A., Boeck, T., Zhao, Y. & Zikanov, O. 2013 Patterned turbulence in liquid metal flow: Computational reconstruction of the Hartmann experiment. *Phys. Rev. Lett.* **110**, 084501.

Krasnov, D., Zikanov, O. & Boeck, T. 2011 Comparative study of finite difference approaches to simulation of magnetohydrodynamic turbulence at low magnetic Reynolds number. *Comp. Fluids* **50**, 46–59.

Krasnov, D., Zikanov, O., Rossi, M. & Boeck, T. 2010 Optimal linear growth in magnetohydrodynamic duct flow. *J. Fluid Mech.* **653**, 273–299.

Krasnov, D. S., Zikanov, O. & Boeck, T. 2012 Numerical study of magnetohydrodynamic duct flow at high Reynolds and Hartmann numbers. *J. Fluid Mech.* **704**, 421–446.

Reynolds, O. 1883 An experimental investigation of the circumstances which determine whether the motion of water shall be direct or sinuous, and of the law of resistance in parallel channels. *Philos. T. R. Soc. A* **174**, 935–982.

Wygnanski, I. J. & Champagne, F. H. 1973 On transition in a pipe. Part 1. The origin of puffs and slugs and the flow in a turbulent slug. *J. Fluid Mech.* **59**, 281–335.

Zikanov, O., Krasnov, D., Li, Y., Boeck, T. & Thess, A. 2013 Patterned turbulence in spatially evolving magnetohydrodynamic tube flows. *Theor. Comp. Fluid Dyn.* Accepted for publication.